Diffraction Methods in the Study of Protein Dynamics and Enzyme Mechanism

Pro Gradu

Esko Oksanen

Laboratory of Organic Chemistry

University of Helsinki

Contents

1. Introduction

Enzymes are biological catalysts that are capable of increasing reaction rates by many orders of magnitude. The ways in which enzyme achieve this is a key question in biology and chemistry and is widely debated. Not surprisingly much effort has been put to understanding enzyme action. Experimental methods such as fast kinetics, FTIR spectroscopy or crystallography are supported by computational approaches.

Diffraction of X-rays, electrons or neutrons by single crystals has provided most of the available information on the structure of biological macromolecules such as proteins and DNA. Due to developments in protein expression, purification and crystallisation, the availability of high intensity synchrotron radiation and also improved software and sufficient computing power, new structures are solved at an ever increasing rate by X-ray crystallography[1].

Any structural investigations of enzymes are usually preceded by extensive biochemical studies. These include the characterisation of the reactions kinetics with either steady-state or stopped or quenched flow methods. Information on the characteristics of the enzyme and its inhibitors or activators is often helpful for successful crystallographic experiments.

The traditional approach to study reaction mechanism with diffraction methods has been to crystallise the enzyme of interest in complexes with competitive inhibitors that are substrate or transition state analogues. Site-directed mutagenesis has also been used to investigate the role of the active site residues. These studies have contributed to the understanding of enzyme action and form a solid basis for mechanistic postulations.

One limitation of traditional X-ray crystallography is that the information obtained from a typical crystal structure is mainly of a static nature. This is precisely the reason why stable analogues of reaction intermediates are typically used in crystallographic studies to obtain snapshots along the presumed reaction path. The time scale of a normal diffraction experiment with monochromatic radiation and the oscillation method ranges from minutes at third generation synchrotron sources such as the ESRF (European Synchrotron Radiation Facility, Grenoble, France) to days with conventional X-ray generators. The electron density maps from such experiments represent an average over the molecules in the crystal and over the time scale of the experiment. When an atomic model is refined against the observed structure factor amplitudes, information about the dynamic behaviour is incorporated into the crystallographic temperature factors. The analysis of these temperature factors yields information about the mobility of different regions of

the molecule. Atomic resolution diffraction data allows the refinement of anisotropic temperature factors, from which even more information can be extracted[2]. Such high resolution data also allow the refinement of several alternative conformations that are discernible in the crystal. The alternative conformations may also shed light on mechanisms.

In contrast to these methods in which the dynamics is observed indirectly, time resolved diffraction methods can also be used[3]. One possibility is the white beam Laue technique. It makes use of the polychromatic or 'white' X-radiation available from a synchrotron source. Using a white beam allows a much larger region of reciprocal space to be covered by one image, allowing a structure to be determined from only one image. Such high time resolution makes it possible to e.g. monitor the structural changes during an enzymatic reaction. Another possibility to conduct time-resolved crystallographic experiments is to monitor the progress of a reaction within a crystal with such as UV-VIS or FTIR spectroscopy and cool the crystals at different identifiable states for data collection by the normal monochromatic oscillation method[4].

Various techniques apart from crystallography are available for the investigation of protein dynamics in general and enzymatic catalysis in particular. They are not covered here in depth, merely mentioned. The information obtained by these methods is often essential for the validation of crystallographic data, for its interpretation and planning further experiments.

Time-resolved solution scattering methods can also be used to study biomolecular dynamics, although not at atomic resolution. Small angle scattering experiments with X-rays can provide time resolved information if performed at high flux sources, such as third generation synchrotrons. The incoherent scattering of neutrons can also be used to identify thermal disorder in proteins, thus complementing the time-averaged data available from crystal structures.

Indirect structural information on the active site during catalysis may also be obtained by spectroscopic methods. The most traditional is electronic (UV-VIS) spectroscopy, which unfortunately yields little specific chemical information. Specific data on individual vibrational modes is available through FTIR spectroscopy. The use of difference spectra enables the extraction of the relevant signals, but their identification and correlation to structural changes remains somewhat problematic. Also many other spectroscopic techniques with reasonable signal-to-noise ratios can be used for time resolved experiments, such as EXAFS, EPR or resonance-Raman spectroscopies.

Nuclear magnetic resonance (NMR) spectroscopy is a very useful technique for studying the dynamic behaviour of biomolecules, including domain movements and conformational freedom of individual side chains. Even though NMR is widely used for the study of biomolecular dynamics, it will not be discussed except for purposes of comparison to scattering techniques.

The variety of computational methods used to study the dynamics of biological macromolecules is very large. Classical molecular dynamics is a widely used method to simulate protein dynamics, but it fails to describe processes involving bond formation or cleavage, such as enzyme action. Quantum chemical calculations can be very helpful for a more thorough understanding of enzyme catalysis, since the available experimental methods can rarely provide specific information on electronic structure. The recent developments in both software and hardware have made quantum chemical calculations feasible on systems large enough to be biochemically relevant. Even the incorporation of nuclear quantum effects like tunnelling is becoming possible. Accurate structural information, however, remains a prerequisite for the use of such methods.

2. Brief Summary of Crystallographic Structure Determination

The principles of crystallography are well covered in various textbooks[1,5,6,7,8]. This summary is intended only to refresh the memory of the reader. The reader is strongly urged to consult the literature for a more detailed exposition.

The scattering of X-rays from an infinite, periodic object, such as a crystal (the number of molecules in a normal crystal is so large that it may be considered infinite for most practical purposes), is non-zero only if the scattered waves interfere constructively. The periodicity of a crystal allows the definition of a *lattice* of identical points, connected by *lattice vectors*. These vectors are linear combinations of *basis vectors*, called **a**, **b** and **c**, that define the unit cell. A central concept in crystallography is the reciprocal lattice, in which the basis vectors **a***, **b*** and **c*** are related to the real lattice basis vectors by **a**• **a*** = 1, **b**• **b*** = 1 and **c**• **c*** = 1.

If the incoming wave is represented by a wave vector **k** and the scattered wave by **k'**, the scattered intensity will be non-zero only if **k'-k = h**, where **h** is a reciprocal lattice vector (h **a***, k **b*** , l **c***), such that h, k and l have integral values. This is known as the Laue condition (not to be confused with Laue crystallography). By considering the crystal as a set of planes, one arrives at an equivalent formulation known as the Bragg law; $n\lambda = 2d \sin\theta$, in which λ is the wavelength, θ the angle between the reflecting plane and the incoming beam and d the interplanar spacing.

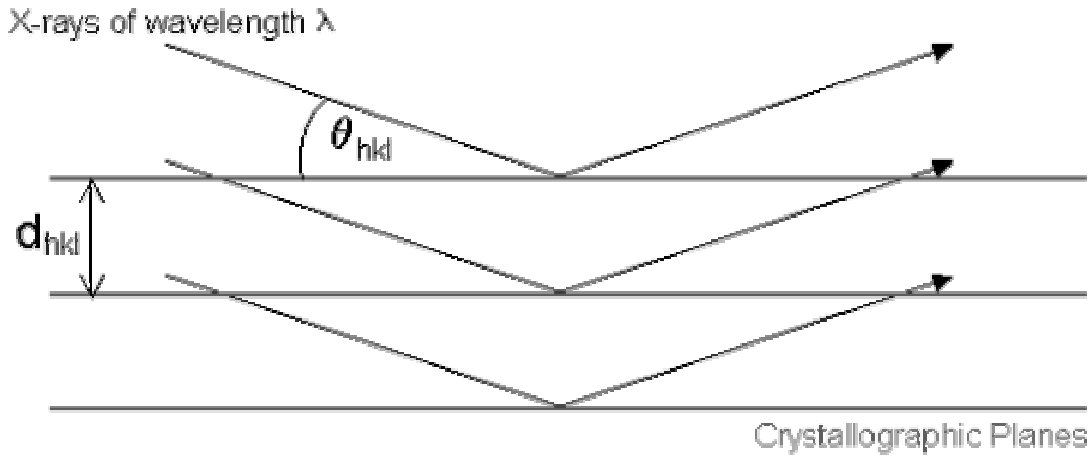

Figure 1 The Bragg law

A common way of describing a diffraction experiment is the Ewald construction. The point Y corresponds to the origin of the reciprocal lattice, point X to an arbitrary reciprocal lattice point h,k,l and A to the X-ray source. The radius of the sphere equals $\frac{1}{\lambda}$. A reciprocal lattice point satisfies the Laue conditions, i.e. is in diffracting position only at the surface of the Ewald sphere.

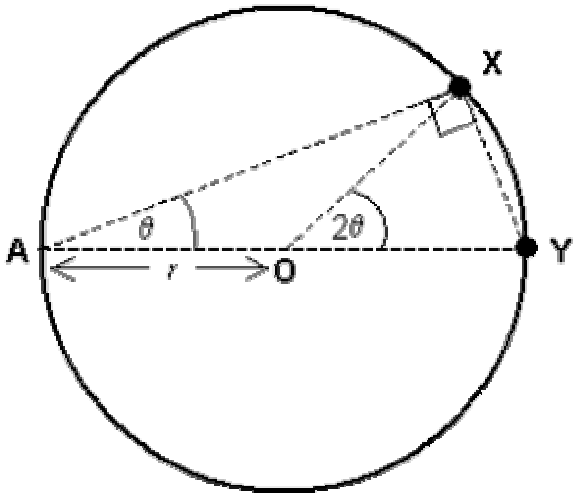

Figure 2 The Ewald construction

The experimental data in crystallography consists of intensities of reflections indexed according to the values of h, k and l. The scattering of X-rays is due to electrons, and the electron density of the crystal can be reconstructed by Fourier synthesis. Unfortunately the phase of the Fourier components, called structure factors **F**(h,k,l), is not measured in the intensities, which are proportional to $|\mathbf{F}(h,k,l)|^2$. Since the phases of reflections dominate the outcome of the Fourier synthesis, they must be obtained in some indirect manner. The most common methods for tackling

the phase problem include multiple isomorphous replacement, single or multiple wavelength anomalous diffraction and molecular replacement. These have been well documented in the literature[1,7,8,9,10].

An atomic model is constructed based on the electron density maps and the atomic coordinates and temperature factors (B-factors) are refined to fit the experimental data as well as possible. The temperature factors model thermal motion and static disorder in the crystal.

2.1. Notes on Electron Density Maps and their Interpretation

The structural information from a crystal structure comes from the interpretation of the electron density maps calculated by Fourier synthesis. The appearance of these maps, which determines their interpretability, is dominated by the phases. The phases cannot be directly measured and the error in the phases is difficult to estimate. Another source of error is the fact that the electron density represents an average over the time for data collection and over all the molecules in the crystal that are considered identical (i.e. related by crystallographic symmetry operations). The phases are normally calculated from an atomic model, where static and dynamic disorder is modelled with B-factors. In truly atomic resolution structures, alternative models can be used and their occupancies refined, but this is usually limited in scope to individual side chains or loops.

A problem associated with phases calculated from a model is model bias. Since the phases dominate the appearance of the electron density map, incorrect features present in the model may appear in the map. For this and other reasons simple Fourier maps are rarely used in crystallography. Various kinds of difference maps, often denoted F_o-F_c-maps, are used to judge the consistency of the model and the observed amplitudes. F_o stands for observed structure factor amplitudes and F_c for amplitudes calculated from the model. A Fourier synthesis with these coefficients produces a map in which positive density indicates features present in the data, but not in the model, whereas negative density indicates features that are present in the model, but not in the data. Since the phases (from the model) are not perfect, such difference maps tend to be rather noisy and are often difficult to interpret. Difference maps can also be calculated from amplitudes originating from two different crystals. Such difference maps have been used to locate inhibitors bound to enzymes by measuring data with and without soaking the crystal in a solution of the inhibitor and calculating a difference map with the phases from the free enzyme.

The concept of crystallographic resolution in has a precise meaning; the smallest observed Bragg plane separation d_{min}. A common misconception is that the quality and reliability of a structure would be determined solely by the resolution. Since the quality and interpretability of the maps is dominated by the phases, it is the quality of the phases that is often crucial. It is also possible that some regions of the molecule are disordered and hence poorly or not at all modelled. This can occur even in structures considered to have high resolution.

3. Time averaged dynamics

Since the time scale of a typical monochromatic diffraction experiment is typically hours or days and the time scale of protein dynamics is femtoseconds to milliseconds, the crystal structure represents an average over time and the molecules in the crystal. It turns out that this information can be extracted and used for a better understanding of protein dynamics and function.

3.1. Crystallographic temperature factors

Atoms in a crystal are not perfectly ordered, but exhibit both static and dynamic disorder. The static disorder results from the breakdown of crystal symmetry, i.e. not all atoms are in equivalent positions. Dynamic disorder is due to the vibrations of atoms (and larger aggregates of atoms, such as entire molecules) around their equilibrium position. The two different sources of disorder cannot normally be separated, as this would require temperature dependent measurements[9]. The way in which this disorder is modelled in the crystal structure is by B-factors, also known as Debye-Waller-factors.

Assuming the scattering of X-rays is centred on atoms, the structure factor of a reflection with indices h,k,l is $\mathbf{F}(\mathbf{h}) = \sum_j f_j \, e^{2\pi i(\mathbf{h}\bullet\mathbf{x}_j)}$, where f_j represents the atomic scattering factor, **h** is the reciprocal lattice vector h,k,l and $\mathbf{x_j}$ is the coordinate vector of atom j. The B-factor is an exponential attenuating factor associated with each atomic scattering factor $f_B = f_0 e^{-B(\sin\theta/\lambda)^2}$, where θ is the scattering angle and λ the wavelength. The B-factor is related to the mean square displacement (MSD) $\langle u^2 \rangle$ of the atom by $B = 8\pi^2 \langle u^2 \rangle$. In typical protein structure refinements, the atomic displacements are assumed to be isotropic, i.e. the probability distribution is spherical. In

reality the movements of atoms rarely are isotropic; anisotropic disorder can be modelled by replacing the B-factor, which is a scalar (or more formally a tensor of zeroth rank), with a 3×3 matrix (or tensor of second rank). A 3×3 matrix has nine elements but, since it is a tensor, only six elements are independent[10]. The anisotropic displacement matrix U_j of atom j is symmetric and its diagonal elements represent the variances of each coordinate value and the off-diagonal elements the respective covariances. $U_j = \begin{pmatrix} u_1^2 & u_1u_2 & u_1u_3 \\ u_1u_2 & u_2^2 & u_2u_3 \\ u_1u_3 & u_2u_3 & u_3^2 \end{pmatrix}$ The elements of the U-matrix are referred to as anisotropic displacement parameters (ADPs). In small molecule crystallography anisotropic Us are routinely used, since the data extends to atomic resolution and the five additional parameters to be refined per atom are not a problem. In proteins, however, the resolution is usually 'near atomic' and the number of parameters needed for anisotropic Us easily exceeds the number of observed reflections. Therefore only structures with resolution higher than 1.2 Å are usually refined with anisotropic Us[11].

The anisotropic displacement parameters are usually represented graphically by ellipsoids defined by the eigenvectors (or principal axes) of the U-matrix. Since the U-matrix is a tensor, it has to be positive definite and hence its eigenvectors do define an ellipsoid instead of other conics.

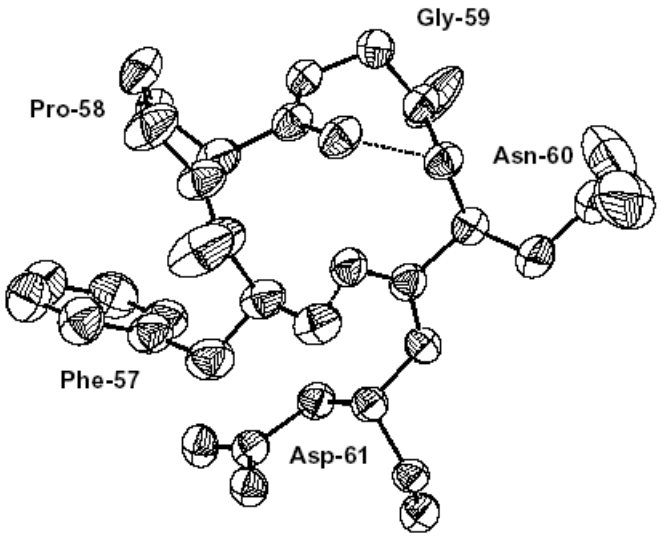

Figure 3 A loop region from a serine protease, illustrating anisotropic displacement ellipsoids

In macromolecular crystallographic structure refinements the values of parameters are usually restrained based on prior chemical knowledge. The restrains used for ADPs for instance in the program SHELXL[12], which is often used in atomic resolution refinements, ensure that the

dynamic behaviour of bonded atoms is similar. For example the shape and direction of the thermal ellipsoids are restrained to be similar (the DELU and SIMU restraints in Figure 4). For waters and hydrogens (which can be modelled in high resolution structures) it is usual to impose isotropic restrains to avoid fitting physically unreasonable models.

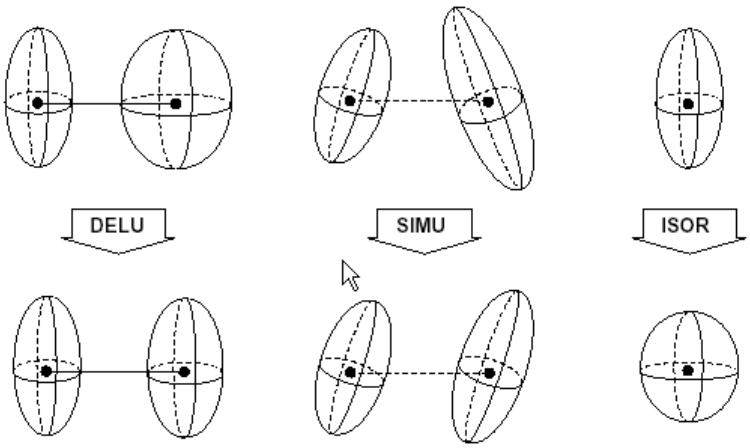

Figure 4 The restraints used for anisotropic displacement parameters in the program SHELXL[2,33]

3.2. The TLS model

The static and dynamic disorder present in crystals is rarely manifested in random, non-correlated movements of individual atoms. Instead, movements of entire molecules or relatively rigid domains within molecules are more likely. It is possible to describe any movement of a rigid body with three matrices[13,14]; **T** (for translation), **L** (for libration) and **S** (for screw). **T** and **L** matrices are symmetric, whereas **S** is not. The application of these matrices allows the calculation of anisotropic displacement factors. The difference between the values calculated for the TLS model and individual atoms is minimised by varying the elements of the **T**, **L** and **S** matrices, thus resulting in a best fit of the rigid body displacement parameters. Incidentally, the same formulation can also be used in refinements which do not allow individual anisotropic displacement parameters to be fitted. This so called TLS-refinement[15] fits rigid body displacement parameters to individual molecules or domains (as defined by the user), thus drastically reducing the number of parameters to be fitted. Whichever way the TLS parameters are obtained, one should always try to assess whether the rigid body assumption actually is valid and physically reasonable. One obvious way is to visualise the principal axes of the matrices. The rigid domains can also be identified, either prior to TLS analysis, or afterwards for its validation, by analysing interatomic differences in displacements. If two atoms A and B belong to a rigid body, their displacements along the

interatomic vector should be the same. The difference Δ_{AB} of the displacements should therefore be zero within experimental error. The n×n matrix, where n is the number of atoms formed by these Δ-values is known as the Δ-matrix[16]. For even a small protein the calculation of the full Δ-matrix is neither feasible nor very helpful.

$$\begin{aligned}\Delta_{AB} &= \left\langle u_A^2 \right\rangle_{\hat{n}} - \left\langle u_B^2 \right\rangle_{\hat{n}} \\ &= \hat{n}^t \mathbf{U}_A \hat{n} - \hat{n}^t \mathbf{U}_B \hat{n} \\ &\approx 0\end{aligned}$$

Figure 5 Displacements of two atoms belonging to a rigid body

Consequently the Δ-matrix is usually calculated for suitable subsets of atoms, such as C_α atoms. Even including only C_α atoms of a protein would result in a huge matrix, so the Δ values are binned to represent larger groups of atoms. Once the validity of the TLS model has been assessed, the biological relevance of the pseudo-rigid body motion can be interpreted with more confidence. It is also important to take into account the effect of the restraints on ADPs in the structure refinement.

3.3. Applications of TLS Analysis

Although the underlying theory has been known for decades and is widely used in small molecule crystallography, the applications to protein crystallography are mostly quite recent. This may be due partly to the lack of atomic resolution data with anisotropic displacement factors and partly to the lack of software to easily perform such analysis.

One early example is the study on ribonuclease A at 1.45 Å resolution[17], in which the movements of side chains as well as the entire molecule were analysed with the TLS model. While the movement of the whole molecule was mostly translational and isotropic, the side chains on the surface had librational movements. In the protein core the motion followed more that of the environment and hence was mostly translational.

Arginine kinase catalyses a reversible phosphoryl transfer between adenosine triphosphate (ATP) and arginine. A crystal structure of the enzyme was solved for a complex with ADP (adenosine diphosphate) and nitrate which mimic the postulated trigonal transition state[18]. The 1.2 Å resolution of the structure allowed the refinement of ADPs and fitting of a TLS model of four domains as rigid bodies. The domains were identified from the Δ-matrix. The movement of these

domains is largely librational, while the domains with catalytically important residues have least mobility. The binding of the transition state analogue also restricts the domain movements

Calmodulin is a calcium-binding protein involved in regulation of other proteins. A structure of calmodulin with Pb^{2+} instead of Ca^{2+} is significantly more disordered and diffracted only to 1.75 Å resolution instead of 1.0 Å[19]. Despite this a TLS model revealed relatively large anisotropic librational movements of the two TLS-groups in the N-terminal domain not observed in the Ca^{2+} containing structure. These movements constitute a complex opening-closing domain motion. This view is also supported by analysis of Δ-matrices.

Phospholipase A2 is an enzyme that hydrolyses the 2-acyl ester bond of 1,2-diacylglycero-3-phospholipids. The bovine pancreatic enzyme has been solved at 0.97 Å resolution but no TLS analysis was performed[20]. The bacterial enzyme from *Streptomyces violaceoruber* was solved at 1.05 Å resolution and the TLS analysis of the bovine enzyme was performed and compared to the bacterial enzyme[21]. This structure is remarkable because the data collection was done in room temperature with a conventional rotating anode generator. Most crystals require cryo-cooling and synchrotron radiation to diffract to atomic resolution. Therefore the displacement factors in this structure are more due to thermal motion than positional disorder. The bovine protein was, however, collected at a cryotemperature, and yet the disorder appeared at the same residues. This suggests that the disorder is broadly similar in cryo and room temperatures, which is encouraging as most crystals are cryocooled for data collection. An interesting comparison is also made between the information obtained from an NMR and a crystal structure. For comparison purposes an anisotropic displacement factor was calculated from the NMR ensemble with the formula $U_{ij}^{NMR} = \left\langle \left(r_i - \left\langle r_i \right\rangle \right) \left(r_j - \left\langle r_j \right\rangle \right) \right\rangle$, where r_i is the i-coordinate of an atom in one conformer of the ensemble, $< r_i >$ is its average and i and j are x, y or z. Most of the residues deemed to be mobile in NMR had high displacements in the crystallographic model, even though the magnitude of the displacement was smaller in the crystallographic model. This would indicate that the molecule has more flexibility in solution than in the crystal. However, the N-terminal region, believed to be involved in substrate binding, that was mobile in NMR, did not show signs of being disordered in the crystal. However, the structure is also different in the crystal and in solution, so it is assumed to be an example of preferential crystallisation of one conformer.

Human fibroblast growth factor 1 was solved at 1.1 Å resolution and refined with anisotropic temperature factors[22]. Rigid domains were identified from the Δ-matrix and TLS analysis performed. The domain definitions were then optimised by repeating the TLS analysis with

various definitions and selecting the best fitting one. The β-strands in the C-terminus seem to move as a rigid body, while the N-terminal β-strands move more or less independently.

The chaperonin GroEL is a large protein assembly that mediates protein folding. The co-chaperonin GroES participates in the 'catalytic' cycle, which is driven by the hydrolysis of ATP. In a study that combined 'chemical trapping' with TLS refinement[23], GroEL was crystallised alone, with ATPγS (unhydrolysable analogue of ATP), ADP and GroES, ADP-AlFx and GroES (a transition state analogue of ATP hydrolysis). Even though the resolutions of the structures range from 2.0 to 3.0 Å, the TLS parameters fitted in structure refinement are consistent between the structures and improved the model. Furthermore, the directions of the rigid body movements are consistent with the differences of domain orientations between the structures, and help to from a picture of the dynamics of the complex.

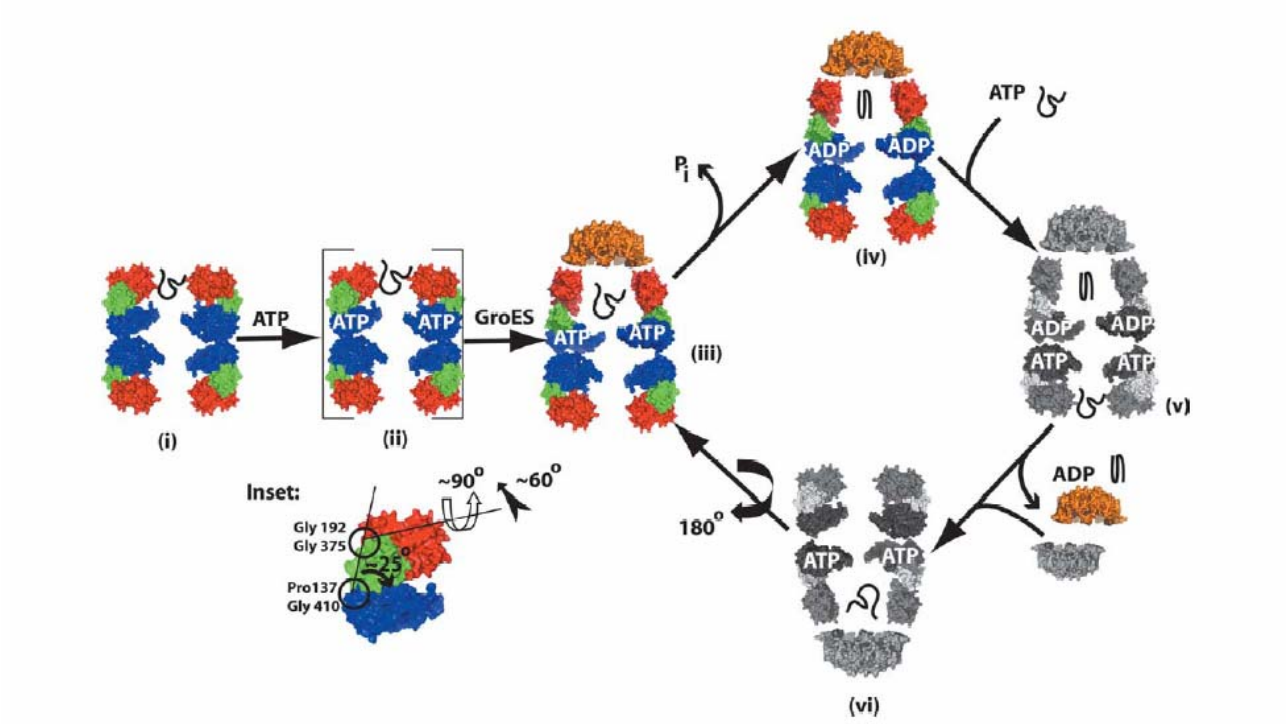

Figure 6 Schematic representation of the domain movements in the GroEL-GroES system. The black line represents an unfolded polypeptide, the GroEL domains are in red, green and blue and GroES in orange.

The bacterial light-harvesting complex II (LH2) is an assembly of proteins, bacteriochlorophyll and carotenoids. It is an integral membrane complex that captures photons and transfers the excitation energy on to a photosynthetic reaction centre. A crystal structure was solved at 2.0 Å resolution and a TLS refinement significantly improved the quality of the model[24]. The domain motions are consistent with spectroscopic results and represent an improvement over stochastic models of thermal motion.

These examples illustrate the potential of the rigid body TLS model in extracting meaningful dynamic information from static crystal structures. While atomic resolution data is clearly advantageous, it is not strictly necessary for the use of the TLS model, thus enabling studies of large complexes or membrane proteins. In these cases the importance of the validation of the model and checks of physical reasonability are particularly pronounced.

4. Time-Resolved Crystallography

Time-resolved crystallography attempts to obtain structural information in time scales shorter than that of the dynamic process of interest. This dynamic process is often an enzymatic reaction, but it may well be any other change of atomic coordinates. It should be noted that transition states in enzymes can not be observed with crystallographic techniques. A transition state corresponds to a saddle point in the multidimensional potential energy surface of a reaction. A saddle point is a potential energy maximum along the reaction coordinate and a minimum along all other coordinates. For a chemical reaction the reaction coordinate usually corresponds to some vibrational mode of the system. Hence the lifetime of a transition state is in the order of one vibrational period, typically in the picosecond scale. In fact only very specialised experimental methods using femtosecond laser pulses are capable of directly observing transition states[25].

4.1. General Requirements for Time-Resolved Crystallography

If one wants to follow the course of an enzymatic reaction within a crystal with a given time resolution, one of the first questions is that of synchronisation. A fairly recent review by Stoddard[26] addresses this question thoroughly. In order to observe a single, distinct species in the crystal, that species has to have ~90 % occupancy. This imposes the requirement that the reaction needs to be triggered by a process with a rate constant larger than that of the actual reaction.

A clear distinction should be made between reversible and irreversible photochemical processes. Proteins such as bacteriorhodopsin (bR) or photoactive yellow protein (PYP) undergo photocycles, which can be repeatedly observed in one crystal[27]. Such multiple turnover experiments allow better signal-to-noise ratios as the data can be collected and averaged over multiple cycles. Another well-studied example is that of carboxymyoglobin. The CO molecule bound to the heme may be dislodged by laser photolysis, after which it will diffuse back to the binding site via various

intermediates in time frames ranging from pico to milliseconds[28]. On the other hand, most enzymatic reactions are not reversible in a way that would allow repeated observations from one crystal.

Single turnover experiments are less straight forward to perform, but are nonetheless possible. The majority have been performed using photolabile substrate precursors. For very slow reactions diffusion of the substrate into the crystal can be used. According to Stoddard, the saturation of a protein crystal of typical size with substrate requires 15-100 seconds. This would require that k_{cat} of the enzyme would be $< 10^{-3}$ s^{-1} in order to achieve synchronisation, which is very slow for an enzyme in solution. However, the reaction rate in the crystal is usually slower than that measured in solution. Crystallographic flow cells can be used to measure the actual steady-state kinetics in a crystal[29]. If some particular intermediate along the reaction pathway is long-lived enough, it can be visualised, as with cytochrome c peroxidase. The structure of the doubly oxidised state, so called compound I, could be investigated by saturating the crystals with hydrogen peroxide in a flow cell. The presence of this intermediate for some 30 minutes was verified by microspectrophotometry[30].

In the case of trypsin a pH jump has been used to study the acyl-enzyme complex formed between Ser195 and p-guanidinobenzoate. The raising of pH in the crystal allows the putative nucleophilic water molecule to move in position and this process was observed with Laue crystallography[31].

By far the most common method to synchronise enzymatic reactions in crystals is by photolysis of a photolabile substrate precursor. Such precursors are often termed ‘caged’ compounds. Modern, commercially available lasers can routinely produce pulses with nanosecond duration. With optical parameter oscillators wavelength tuneability and narrow band pass are achieved. Even femtosecond laser pulses can be produced, so the excitation has very high time resolution. Once an appropriate photolabile precursor compound is available, certain requirements have to be met for successful time-resolved diffraction experiments. Firstly the rate of the photolytic cleavage has to be as fast or faster than the enzymatic reaction to be studied. Secondly the quantum yield of the process needs to be high enough, so that essentially all the molecules in the crystal can be cleaved with a single laser pulse. Finally the wavelength of the excitation radiation should be easy to produce and should not cause significant damage to the protein.

The most common way of obtaining photolabile precursor compounds is to synthesise a (2-nitrophenyl)-2-ethyl (or o-nitrophenylethyl) derivative. 3,5-dinitrophenyl and similar derivatives have also been used.

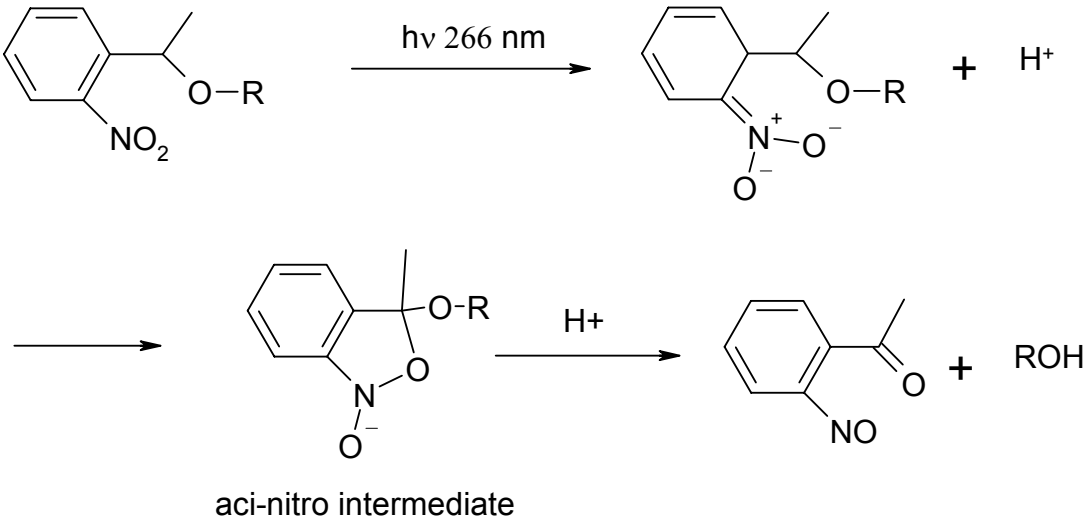

Figure 7 Photolysis mechanism of a *o*-nitrophenylethyl ester

The photolysis of *o*-nitrophenylethyl esters occurs generally in the millisecond regime with high quantum yield[32]. The mechanism presented in (Fig. 7) is a minimal mechanism, and recent studies by time-resolved IR spectroscopy and quantum chemical calculations suggest that photolytic mechanism is in fact more complicated[33]. The photolysis rates of *o*-nitrophenylethyl caged compounds have usually been measured from the decay of the UV absorption due to the aci-nitro intermediate. This is based on the assumption that the decay rate is equal to the rate of release of the caged compound. The more recent studies cast doubt on this assumption. In addition the pH dependence of the photolysis rate is more complicated than previously thought.

A relatively simple and robust synthetic methodology is available for the synthesis of *o*-nitrophenylethyl esters; examples include 'caged' phosphate[34], 'caged' nucleotides, 'caged' pyrophosphate[35], cholin, the hydrolysis product of the neurotransmitter acetylcholine[36] and the Ca^{2+} channel blockers nifedipine and nisoldipine[37].

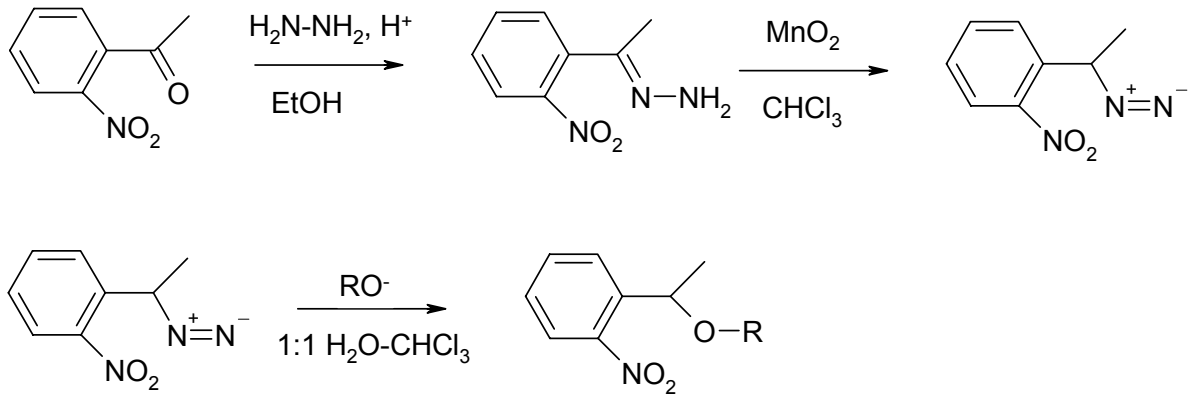

Figure 8 Synthesis of o-nitrophenylethyl esters

It is also possible to genetically incorporate photolabile amino acids, such as *o*-nitrobenzyl cysteine, into proteins using specifically engineered tRNA/aminoacyl tRNA-synthetase pairs[38]. This would allow facile photochemical synchronisation of enzyme reactions dependent on cysteine residues.

The major drawback of *o*-nitrophenylethyl cages is the short wavelength needed to achieve high quantum yield. These UV wavelengths are strongly absorbed by proteins, causing radiation damage and heating problems (especially relevant in cryocrystallographic applications). The absorption also limits the maximum thickness of a sample in which the photolysis can be performed. This problem is of course more pronounced at the high protein concentrations that occur in crystals. The photolysis rates of *o*-nitrophenylethyl compounds are in the millisecond range, which is a result of the various 'dark' steps occurring after the absorption of a photon. Compounds photolysable with longer wavelengths and with faster photolysis rates have been developed, mainly to release amino acid neurotransmitters like glycine or β-alanine. The caging groups include 2-oxo-1,2-diphenylethyl[39] (or desyl), 2-methoxy-5-nitrophenyl[40] (MNP) and 2-(dimethylamino)-5-nitrophenyl[41] (DANP) moieties. The synthesis of such compounds is more complicated than for *o*-nitrophenylethyl esters, and as the caging groups become bulkier and less water soluble, their usefulness for triggering reactions in crystals decreases.

4.2. Trapping Catalysis Intermediates

A common approach to study the structure of intermediates along the catalytic pathway of an enzyme is to prepare indefinitely stable chemical analogues of the intermediates. These analogues can then be crystallised with the enzyme and data collected with the monochromatic oscillation method. This approach is referred to as 'chemical trapping'[42]. For instance, in the case of dihydrofolate reductase six compounds were used to emulate the catalytic intermediates and transition states[43]. An another example is inorganic pyrophosphatase, for which the substrate complex is captured by inhibiting the hydrolysis with fluoride and two different alternate conformations are observed for a high resolution product complex with phosphate. These two conformations are thought to correspond to an immediate and a relaxed product complex[44]. Additional mutant studies of the active site support the model of catalysis[45]. These studies illustrate the range of information available from chemical trapping. The major problem associated with this approach is the assumption that the stable analogues are indeed analogous to actual intermediates

and transition states. Hence the ultimate verification of such mechanistic postulations has to come from structures of actual intermediates.

An alternative way of increasing the lifetime of reaction intermediates is by 'physical trapping', which usually refers to reducing the temperature so much, that the intermediates are stable in the time scales required for diffraction data collection. Two different approaches are available, known as 'freeze-trapping' and 'trap-freezing'. In freeze-trapping the reaction initiation is performed photochemically at cryogenic temperatures. The reaction is greatly slowed down, and specific intermediates can be accumulated by temporarily warming the crystals. Thymidylate kinase, which catalyses the phosphorylation of TMP (thyminosine monophosphate) to TDP (thyminosine diphosphate) was investigated with this method[46]. The appearance of a phosphate group next to the TMP molecule could be observed. Trap-freezing refers to a technique in which the reaction in the crystal proceeds at room temperature, whatever the method of synchronisation may be, and the crystal is flash-cooled to a cryogenic temperature at a specific time point. The catalytic mechanism of the hammerhead ribozyme (catalytic ribonucleic acid molecule) has been studied with a trap-freeze approach[47]. The hammerhead ribozyme cleaves itself, requiring divalent metal ions like Mg^{2+} for catalysis. The reaction does not occur at low pH, and it is fairly slow. Therefore both pH and Mg^{2+} concentration can be used to trigger the reaction, and several intermediates could be accumulated and captured by flash-cooling. It should be noted that the time resolution of this method is ultimately limited by the rate of cooling of the crystal. For a large protein crystal it may take almost 1 s to reach cryogenic temperatures[48]. In some earlier studies of intermediate trapping the crystals were cooled to moderate temperatures to slow the reactions down. The mother liquor was kept liquid by the use of cryoprotectants. Examples include a study on the serine protease elastase, in which the formation of an acyl-enzyme intermediate could be observed[49].

All the approaches outlined above can be combined with the use of specific mutants designed to slow the reaction down at some steps and increase the lifetime of intermediates. Should it not be possible to extend the lifetime of the intermediates enough to allow normal monochromatic data collection, faster crystallographic methods, such as Laue diffraction have to be applied. Such trapping approaches may also make it possible to perform time-resolved neutron crystallography experiments[50]. Neutron crystallography allows the direct observation of protons, which are not usually visible even in high resolution X-ray structures. As protons are crucial for many enzymatic reactions, this would be a valuable addition to the repertoire of available methods. The experimental difficulties involved are significant, but it is possible to solve neutron structures at cryogenic temperatures[51].

4.3. The Laue Method

Laue crystallography refers to single-crystal diffraction experiments with polychromatic (or 'white') X-rays. Although the very first X-ray diffraction images by Friedrich, Knipping and von Laue were obtained by white X-radiation, most crystallography since then has been performed with monochromatic X-rays. One of the major reasons was that the spectrum of X-rays available from conventional generators has strong peaks due to the electronic transitions of the anode material. The most commonly used has been the copper K_α edge at 1.54 Å. With synchrotrons this problem is no longer relevant, since the emission from a synchrotron radiation source is polychromatic.

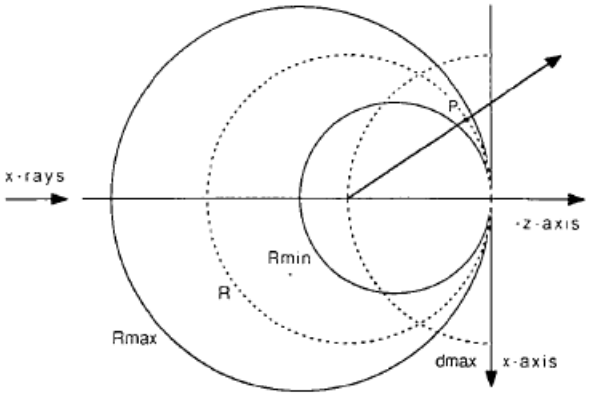

Figure 9 Ewald construction for a Laue diffraction experiment

Figure 5 illustrates the principle of the Laue method in reciprocal space. An Ewald sphere is associated with every wavelength present in the incoming radiation, R_{min} corresponding to the longest and R_{max} to the shortest wavelength present. In reality these can be 'soft' rather than 'hard' limits. The reciprocal lattice point P comes to reflecting position at the wavelength corresponding to a sphere with radius R. The sphere d_{max} is the resolution sphere, determined by crystal quality, which also limits the number of reflections observed. In principle all the reciprocal lattice points in the volume limited by R_{min}, R_{max} and d_{max} are simultaneously in reflecting position.

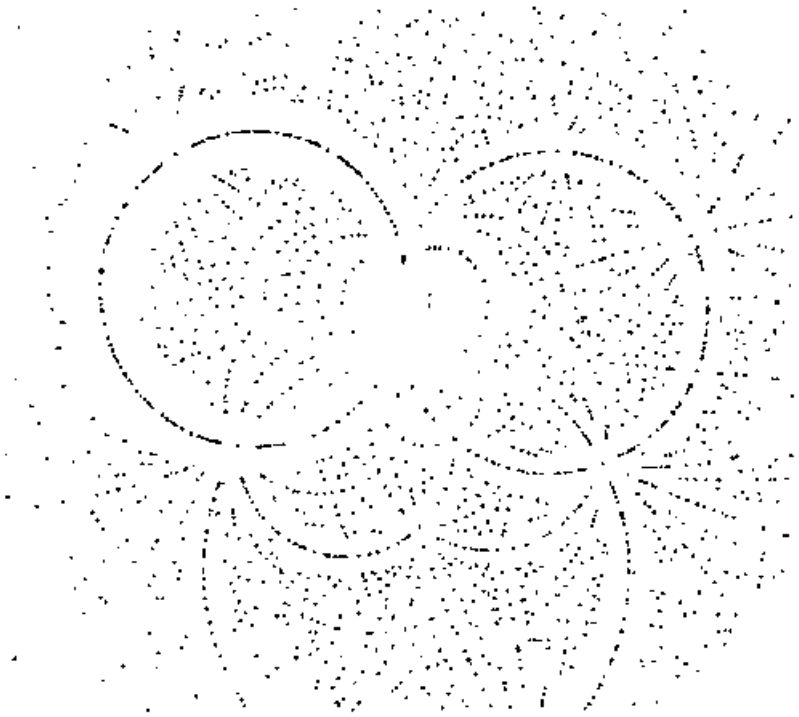

Figure 10 A polychromatic Laue diffraction pattern

The first Laue images of protein crystals were obtained in 1984 at CHESS (Cornell High Energy Synchrotron Source), Ithaca, USA[52]. A serious limitation to the feasibility of Laue crystallography has been difficulty of indexing and integrating the reflections from Laue images. The difficulties result from the large number of overlapping reflections in the images, which need to be deconvoluted somehow. Even the mere indexing of Laue images requires knowledge of either the unit cell dimensions or the crystal orientation. Fortunately the cell dimensions are always known from previous single-wavelength experiments. The problem of harmonic overlaps, i.e. reflections with indices (nh ,nk ,nl), plagues Laue crystallography. However, according to the analysis of Ren *et. al.*[53], the problem is only serious at low resolution. This results from the fact that even though reflections may in theory be in reflecting position, they might not in practice be measurable. In particular the high resolution reflections at short wavelengths, which are most likely to produce harmonic overlaps, are not easily measurable, thereby reducing the number of overlaps. Fig. 11 illustrates the probability distribution of measurable reflections; another observation from this figure is, that the Bragg angle acceptance θ_a is smaller than the Ewald construction alone would suggest.

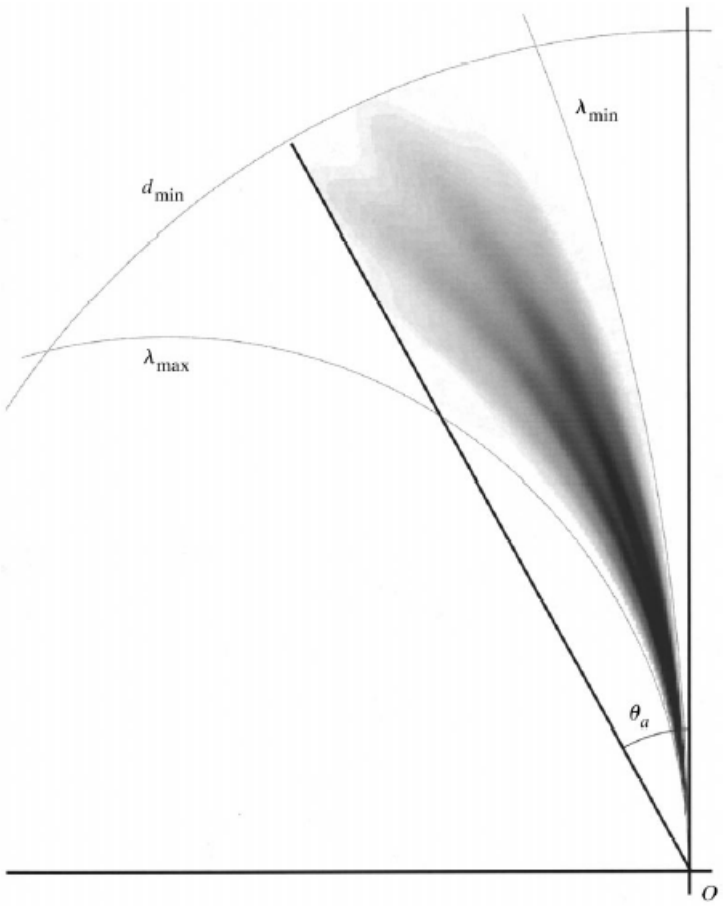

Figure 11 The probability distribution of measurable reflections (for the ID09 beamline at the ESRF)

The lack of the low-resolution terms has an adverse effect to the connectivity of the electron density maps, which hampers their interpretation. The advent of harmonic deconvolution methods have alleviated this problem[54].

Experimental facilities for time-resolved Laue crystallography exist at various synchrotron sources, such as the APS (Advanced Photon Source) in Argonne, USA or the ESRF (European Synchrotron Radiation Facility) in Grenoble, France[55]. The necessary software for data processing is also available, the two most notable software packages being the *Daresbury Laboratory Laue Software Suite*[56] and *LaueView*[22,26].

4.4. Processing of Laue data

The difference between a Laue diffraction experiment and a standard monochromatic experiment is that polychromatic X-radiation is used. The coherent scattering of X-rays by a perfect, infinite crystal is observed only if the Laue conditions are satisfied. The wavevector is

wavelength dependent, its length being uniform in a monochromatic experiment. Hence only a limited number of diffraction spots is observed in any given image, as only a few scattering vectors coincide with reciprocal lattice points. The success of the oscillation method requires sufficient separation of the spots, which allows fairly straight forward indexing and integration of the reflections. The disadvantage is that a fairly large number of 2D images are needed to cover the asymmetric unit of reciprocal space resulting in relatively long data collection times.

If, however, a wide variety of scattering vector lengths is present, a much larger number of reflections will satisfy the Laue conditions. This results in much more crowded images than with monochromatic radiation.

The extraction of reflection intensities from the diffraction images consists of three steps. The first step is indexing. After the positions of diffraction spots (usually spot centroids) are determined, the smallest possible reciprocal lattice basis vectors and the crystal orientation are fitted. The subsequent refinement of these diffraction parameters along with e.g. detector distance yields the information required for the next step, integration. Knowledge of the crystal orientation, unit cell dimensions and X-ray wavelength allows the prediction of reflection positions. The integration of intensity around these predicted spot centroids gives the raw reflection intensities. The background intensity is also estimated around the spots. In the next step, data reduction, different correction factors, such as Lorenz, polarisation or absorption corrections are then applied to the intensities. The intensities are then scaled to absolute scale.

The above applies to monochromatic data as well, but for Laue data additional correction steps are required. Both the actual scattering and the response of detectors depend on wavelength[57]. The scaling stage involves therefore wavelength dependent correction factors. This wavelength normalisation is critical for the structure determination[14]. There are multiple methods for obtaining the so called λ-curve, which describes the wavelength dependence of the source, optics and detector.[58] This can also be used to deconvolute the harmonic overlaps[59]. If a multiple diffraction spot contains a contribution from the reflections F(h,k,l) and F(2h,2k,2l), they may give rise to an observed intensity $I_{obs,a}$ with wavelengths λ_{1a} and λ_{2a}, where $\lambda_{2a} = 2\,\lambda_{1a}$. If the same reflections give rise to an another multiple spot of observed intensity $I_{obs,b}$ with wavelengths λ_{1b} and λ_{2b}, then the observed intensities can be expressed as a pair of equations in terms of the 'real' intensities I_1 and I_2: $\begin{aligned} I_{obs,a} &= g(\lambda_{1a})I_1 + g(\lambda_{2a})I_2 \\ I_{obs,b} &= g(\lambda_{1b})I_1 + g(\lambda_{2b})I_2 \end{aligned}$, where $g(\lambda_i)$ are the wavelength normalisation factors. The deconvolution of n intensities is possible from n observations by solving a set of linear

equations like this. The accuracy of these deconvoluted intensities is therefore strongly dependent on the quality of the wavelength normalisation.

4.5. Analysis of Laue Data

The systems studied with Laue crystallography are usually structurally very well characterised by previous monochromatic experiments. Therefore the solution of the phase problem is rather straight forward with molecular replacement, whereas the interpretation of the electron density maps is less so. The conformational differences between the different intermediates may be small and experimental noise in the map due to e.g. lack of low resolution terms, errors in integrating the intensities or increased crystal disorder lower the signal-to-noise ratio of the map. One strategy to avoid these effects is to perform crystallographic refinement against *differences* in structure factor amplitudes instead of the amplitudes themselves[60]. This is advantageous because much of the noise in the map results from phase error. If the difference map is calculated from two independently refined sets of structure factors, the phase error will add up and reduce the signal-to-noise ratio of the map. This may be avoided by using the same phase and an amplitude difference. The map quality can be further improved with Bayesian weighting schemes for the amplitude differences[61]. Another technique for the improvement of the signal-to-noise ratio is singular value decomposition (SVD), which is another name for eigenvector analysis[62]. The time dependent data in the data matrix **A** is expressed as a function of time-independent, orthonormal basis vectors in matrix **U**, the time dependencies of the corresponding vectors in matrix $\mathbf{V}^T$ and the singular values in matrix **S**. $\mathbf{A} = \mathbf{USV}^T$ The singular values describe how much the corresponding vectors contribute to the data, and can therefore be used to filter out the components that contribute only to noise. A very useful property of the SVD method is that it identifies the largest independent components that change during the time course of the experiment, thus yielding valuable information about the mechanism.

Despite the sophisticated methods used to collect and analyse time resolved crystallographic data, the interpretation of the electron density maps is far from trivial. Due to the nature of the Fourier transformation the way in which experimental errors show in the maps is not straight forward. Hence it is not always easy to distinguish real signals from noise, but despite these difficulties time-resolved crystallography is capable of directly visualising reaction intermediates as the reaction proceeds.

4.6. Some Applications of Time-resolved Laue Crystallography

Much of the development of Laue crystallography has been done on systems which enable multiple turnover. One of the best studied cases is that of the oxygen binding protein myoglobin. It contains a heme prosthetic group which binds carbon monoxide with high affinity. This CO molecule can be photolytically released and the structural relaxation along with the migration of the CO observed with nanosecond Laue crystallography[63,11]. Time-resolved crystallographic studies of myoglobin have also been used to validate molecular dynamics calculations[64]. Figure 13 shows an example of difference electron density from a Laue experiment.

Photoactive yellow protein (PYP) is a photoreceptor of halophilic bacteria. The light-induced isomerisation of the trans-4-hydroxycinnamyl chromophore causes conformational changes that lead to signalling events. The hydrogen bonding network changes upon photoisomerisation, which can be seen with Laue crystallography[10]. The SVD technique has been applied to PYP[31,65].

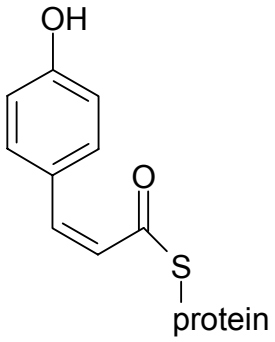

Figure 12 4-hydroxycinnamyl chromophore

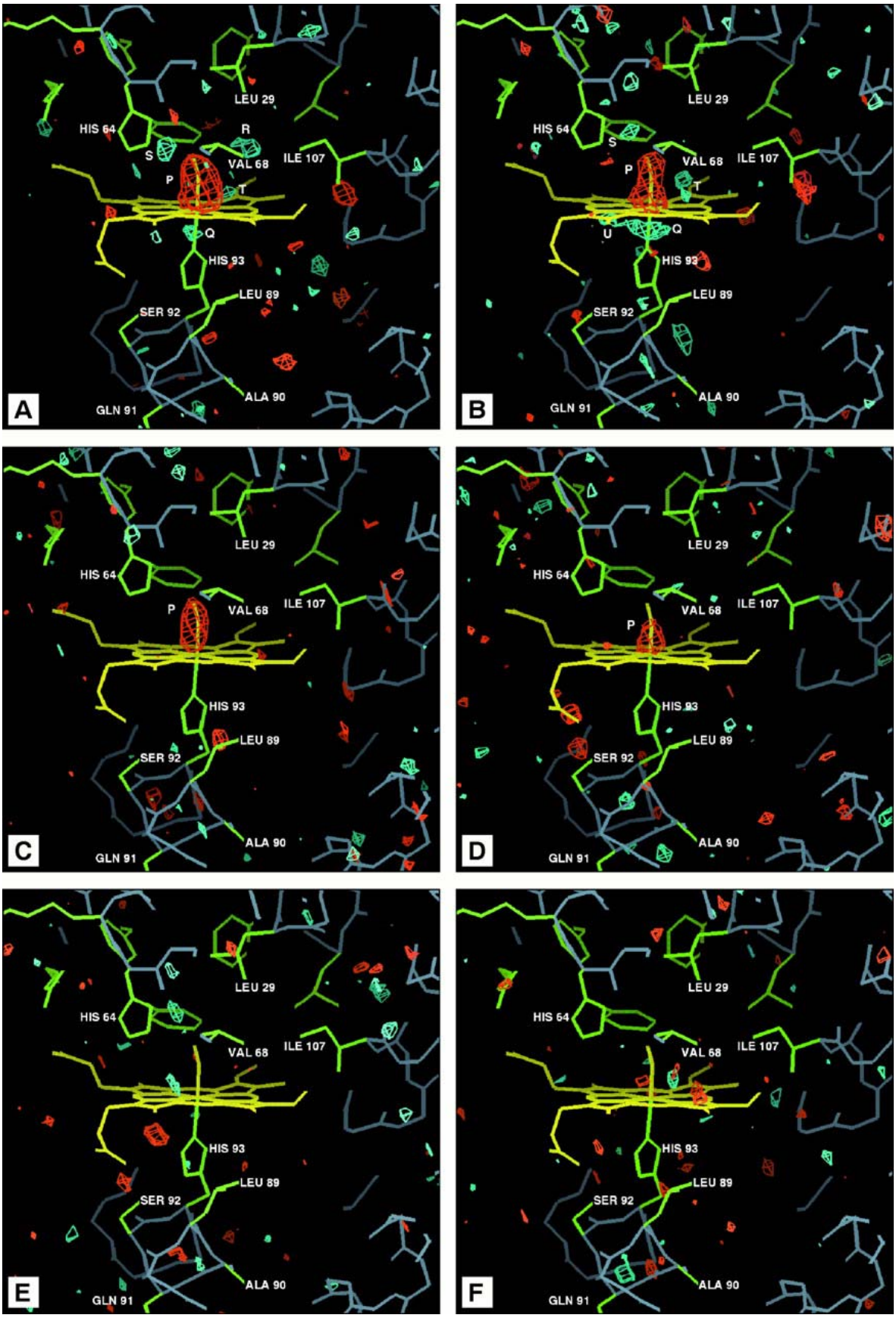

Figure 13 Difference Fourier maps of the heme region in myoglobin after various time delays. Positive contours (density appearing due to photolysis) are shown in green and negative contours (density disappearing due to photolysis) in red. A) 4 ns B) 1 μs C) 7.5 μs D) 50.5 μs E) 350 μs F) 1.9 ms

One of the earliest Laue studies was on glycogen phosphorylase. The binding of the substrate maltoheptose was visualised by calculating a difference map from the Laue data before and after substrate presentation[66]. Later, a photochemically synchronised experiment was performed[67]. The time scale was rather slow, as no phosphorylation of the substrate was observed after 3 minutes, but a distinct phosphate group was seen in the difference map after one hour.

The Ha-ras p21 protein, which is a GTP (guanosine triphosphate) hydrolysing enzyme involved in signal transduction, has also been studied by Laue crystallography[68]. The rate of GTP hydrolysis is relatively slow, making time resolved studies less complicated. The reaction was synchronised by the photolysis of 'caged' GTP. Even though the release of the substrate could be confirmed and conformational changes were seen to take place upon hydrolysis, the difference maps at the active site were inconclusive in the sense that the fate of the γ-phosphate could not be tracked.

For γ-chymotrypsin, which is a serine protease, a photolabile trans-*p*-diethylamino-*o*-hydroxy-α-methylcinnamate was bound to the active site serine[69]. The photolytic cleavage allows the binding of an another inhibitor, 3-benzyl-6-chloro-2-pyrone. This process was observed by Laue crystallography. Despite the additional disorder in the crystals caused by the photolysis, conformational changes in the enzyme active site could be seen.

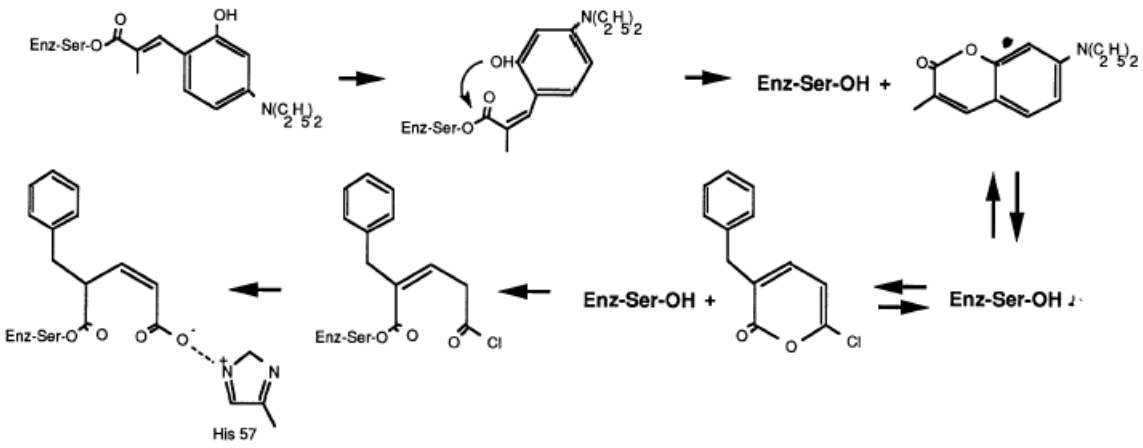

Figure 14 Reaction scheme for the photoinduced binding of 3-benzyl-6-chloro-2-pyrone

Isocitrate dehydrogenase (IDH), which catalyses the oxidative decarboxylation of isocitrate to yield α-ketoglutarate, was investigated by both steady-state and single turnover experiments. The enzyme uses nicotineamide adenine dinucleotide phosphate ($NADP^+$) as an oxidant.

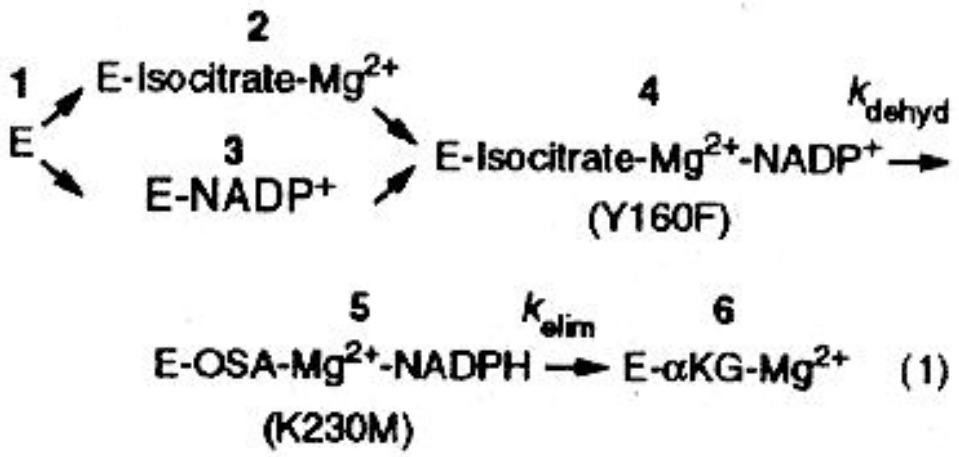

Figure 15 Catalytic scheme of isocitrate dehydrogenase

In the steady-state experiments, the lifetime of catalytic intermediates was increased by suitable active site mutations in order to allow their observation by Laue crystallography[70]. The enzyme-substrate (or Michaelis) complex was captured with the mutation Tyr160Phe and the oxalosuccinate intermediate with Lys230Met.

Hydroxymethylbilane synthase (HMBS) is involved in the biosynthesis of porphyrins (such as hemes) and catalyses the formation of hydroxymethylbilane from four molecules of porhpobilinogen.

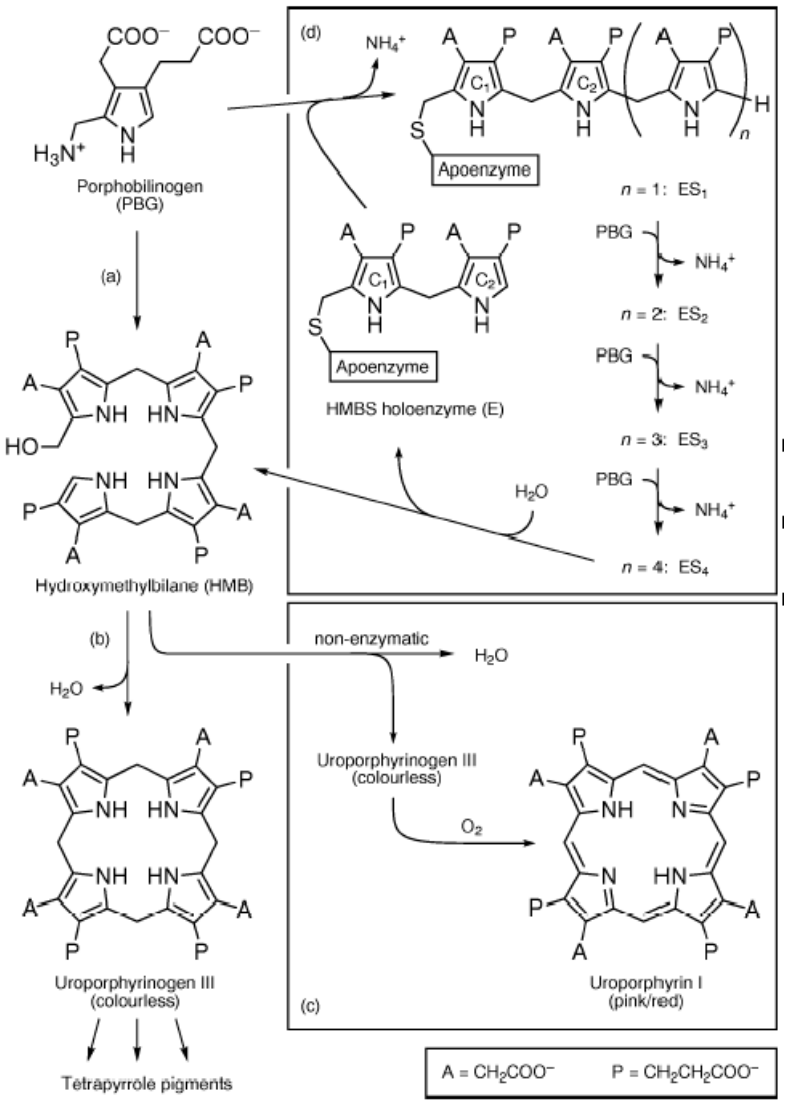

Figure 16 a) Overall reaction catalysed by HMBS b) and c) further metabolism of HMB d) catalytic cycle of HMBS

HMBS forms a sequence of enzyme-substrate complexes, labelled ES_1 to ES_4. The mutant Lys59Gln shows an accumulation of the ES2 complex after some 2 min after reaction initiation. The reaction was performed in a crystallographic flow cell under steady state conditions and followed by Laue crystallography with millisecond exposures[71].

5. Solution Scattering

The scattering of radiation (such as X-rays) by a non-periodic object is continuous in contrast to the sharp diffraction spots from crystals. Since molecules in solution tumble rapidly, the scattering by a molecule in solution is averaged over its rotational trajectory. Hence most atomic

resolution information is lost and only the general size and shape of the molecular object may be inferred. Nevertheless even such low resolution information can be helpful in understanding changes in quaternary structure or detecting large amplitude domain movements. Recent reviews on solution scattering are available[72,73].

The experimental data in solution scattering is the scattering curve as a function of scattering angle. Often only the very low angle scattering is considered, even though the scattering may extend to higher angles. The low angle data contains information about the size and shape of the particle, whereas the high angle scattering results from the internal structure. In contrast to diffraction from crystals, this diffraction data is rotationally averaged and extends to resolutions of 10-5 Å.

Various modelling methods are used to extract information from the solution scattering curve. The most classical one is the Guinier plot which yields the radius of gyration of the particle. More detailed structural information can be obtained by fitting molecular envelopes expressed as an expansion in spherical harmonics to the experimental scattering curve[74]. Various bead models can provide more detailed shape information. The volume defined by the maximum particle diameter is considered as a lattice of points that may contain either protein or solvent. A Monte Carlo simulation is then used to minimize the difference between the scattering calculated from the bead model and the experimental scattering curve. Because the number of beads is much larger than the number of parameters that may reasonably be fitted to the data, constraints must be used in the simulation ensuring continuity and compactness of the model.

Many biologically interesting complexes involve a large number of protein or nucleic acid components. Even if the crystal structures of the individual constituents is known, the entire complex is usually difficult to crystallise and too large for NMR studies. If large amplitude movements are involved in the dynamics, they may be restricted by crystal packing forces or preferential crystallisation of only one conformer may occur. In such problems small angle scattering data can be very useful. It is possible (although not at all trivial) to calculate a solution scattering curve from an atomic model[75]. This allows the fitting of a rigid body motion model to the experimental data. Such a model is basically equivalent to a TLS model discussed earlier, although in the solution scattering case the rigid body postulate is more difficult to verify. However, since the resolution of the data is much lower, it is likely that the postulate is valid for any motions that may be resolved. An example case is aspartate transcarbamoylase, an enzyme that catalyses the first committed step in the biosynthetic pathway of pyrimidines. The enzyme is a heterododecamer and its allosteric regulation by various nucleotides is based on changes in quaternary structure. Solution scattering measurements analysed with a rigid body model showed marked differences in the

quaternary structure in the crystal and in solution[76]. This shows that even though crystal packing is unlikely to significantly change the structure of a folded protein, it may affect the interactions between domains or subunits and constrain their motions.

Solution scattering measurements can also be performed in a time resolved manner. As in diffraction experiments, the factor limiting the time resolution is often synchronisation. Many of the same methods have been used, but diffusion is more practical in solution studies, since rapid mixing devices may be used. High brilliance of the X-ray beam is required for millisecond time resolution and therefore instrumentation for such experiments is available at synchrotron sources, such as the ESRF (Grenoble, France) or ELETTRA[77] (Trieste, Italy). Singular value decomposition (SVD) methods similar to those described above can be used in the analysis of time dependent solution scattering data. This technique allowed the characterisation of an intermediate state in the refolding of the electron carrier protein cytochrome c[78].

Data from solution neutron scattering experiments complements X-ray scattering data. Scattering of neutrons is due to atomic nuclei instead of electrons, and consequently neutron scattering lengths of elements can be radically different from X-ray scattering factors. The large difference in the scattering lengths of ^{1}H and ^{2}H is particularly useful. ^{1}H actually has a negative scattering length, which means that the contrast difference between hydrogenated and deuterated materials is pronounced. This allows contrast variation studies in which the scattering curve is measured in solutions of different H_2O/D_2O ratios. The most remarkable application of solution neutron scattering is the modelling of the ribosome based on solution scattering curves with X-rays and neutrons and contrast variation by selective deuteration[79]. The results were later confirmed by crystallography[80].

6. Comparisons Between Dynamics Information from NMR and Scattering Methods

NMR spectroscopy is based on the energy level difference that a magnetic field causes between the spin states of nuclei. These spin states and coherences between them can be manipulated with radiofrequency pulses. NMR spectroscopy is treated in various textbooks[81]. It is a versatile method that yields information on dynamics in time scales from picoseconds to hours. The investigation of dynamics in the faster regime is usually based on relaxation times. Rates of exchange between conformations with different chemical shifts can be measured for instance by the CPMG (Carr-Purcell-Meiboom-Gill) or $R_{1\rho}$ pulse sequences. These methods have been used to

study the active site dynamics of enzymes, such as cyclophilin A[82] or the ribonuclease binase[83]. In both cases the time scale of the active site motions during catalysis corresponded to the reaction rates. Since the information obtained from NMR is time-averaged, it compares with the information in crystallographic temperature factors, although NMR experiments are capable of charactering the time scale of the motions. NMR does not provide information similar to time resolved crystallography and scattering methods, where the progress of an enzymatic reaction can be directly visualised.

References

[1] Giacovazzo, C., Monaco, H.L., Artioli, G., Viterbo, D., Ferraris, G., Gilli, G., Zanotti, G., Catti, M. *Fundamentals of Crystallography, 2nd Edition*, Oxford University Press (2002) Oxford, U.K.

[2] Schneider, T.R. (1996) *Proceedings of the CCP4 Study Weekend* (eds. Dodson, E., Moore, M., Ralph, A., and Bailey, S.), SERC Daresbury Laboratory, Daresbury, U.K., 133-144

[3] Moffat, K. *Acta Cryst.* (1998) A**54**, 833-841

[4] Stoddard, B.L. *Methods* (2001) **24**, 125-138

[5] Drenth, J. *Principles of Protein X-Ray Crystallography, 2nd Edition,* Springer Verlag (1999) New York, USA

[6] Blow, D. *Outline of Crystallography for Biologists*, Oxford University Press (2002) Oxford, UK

[7] McRee, D. *Practical Protein Crystallography, 2nd Edition*, Academic Press (1999) San Diego, USA

[8] Rhodes,G. *Crystallography made crystal clear, 2nd Edition*, Academic Press (2000) San Diego, USA

[9] Bürgi, H.B., Capelli, S.C., *Acta Cryst.* (2000) A**56**, 403-412

[10] Sands, D.E., *Vectors and Tensors in Crystallography*, Addison-Wesley (1982) Reading, USA

[11] Dauter, Z., Lamzin, V.S., Wilson, K.S., *Curr. Opin. Struct. Biol*. (1997) **7** 681-688

[12] Sheldrick, G.M., Schneider. T.R., *Methods Enzymol.* (1997) **276,** 307-326

[13] Cruickshank, D.W.J, *Acta Cryst.* (1956) **9,** 754-756

[14] Schomaker, V, Trueblood, K., *Acta Cryst.* (1968) B**24**,63-76

[15] Winn, M.D., Isupov, M.N., Murshudov, G.N., *Acta Cryst.* (2001) D**57,** 122-133

[16] Rosenfield, R.E., Trueblood, K.N., Dunitz, J.D., *Acta Cryst.* (1978) A**34,** 828-829

[17] Howlin, B., Moss, D.S., Harris, G.W., *Acta Cryst.* (1989) A**45**, 851-861

[18] Yousef, M.S., Fabiola, F., Gattis, J.L., Somasundaram, T., Chapman, M.S., *Acta Cryst*. (2002) D**58**, 2009-2017

[19] Wilson, M.A., Brunger, A.T., *Acta Cryst.* (2003) D**59**, 1782-1792

[20] Steiner, R.A., Rozeboom, H.J., de Vries, A., Kalk, K.H., Murshudov, G.N., Wilson, K.S., Dijkstra, B.W., *Acta Cryst.* (2001) D**57**, 516-526

[21] Matoba, Y., Sugiyama, M., *Proteins: Struc. Funct. Genet.* (2003) **51**, 453-469

[22] Bernett, M.J., Somasundaram, T., Blaber, M., *Proteins: Struc. Funct. Bioinf.* (2004) **57**, 626-634

[23] Chaudhry, C., Horwich, A.L., Brunger, A.T., Adams, P.D., *J. Mol. Biol.* (2004) **342**, 299-245

[24] Papiz, M.Z., Prince, S.M., Howard, T., Cogdell, R.J., Isaacs, N.W., *J. Mol. Biol.* (2003) **326**, 1523-1538

[25] Paik D.H., Yang D.S., Lee I.R., Zewail A.H., *Angew. Chem. Int. Ed. Engl.* (2004) **43**(21), 2830-2834

[26] Stoddard, B.L. *Pharmacol. Ther.* (1996) **70**(3), 215-256

[27] Genick, U.K., Borgstahl, G.E., Ng, K., Ren, Z., Pradervand, C., Burke, P.M., Srajer, V., Teng, T.Y., Schildkamp, W., McRee, D.E., Moffat, K., Getzoff, E.D., *Science* (1997) **275**, 1471-1475

[28] Bourgeois, D., Vallone, B., Schotte, F., Arcovito, A., Miele, A.E., Sciara, G., Wulff, M., Afinrud, P., Brunori, M., *PNAS* (2003) **100**(15), 8704-8709

[29] Stoddard, B.L, Farber, G.K., *Structure* (1995) **3** 991-996

[30] Fülöp, V., Phizacerley, R.P, Soltis, S.M., Clifton, I.J., Wakatsuki, S., Erman, J., Hajdu, J., Edwards, S.L. *Structure* (1994) **2** 201-208

[31] Singer, P.T., Smalås, A., Carty, R.P., Mangel, W.F., Sweet, R.M., *Science,* (1993) **259**, 669-673

[32] Walker, J.W., Reid, G.P., McCray, J.A., Trentham, D.R., *J. Am. Chem. Soc.* (1988) **110**, 7170-7177

[33] Il'ichev, Y.V., Schwörer M.A., Wirz, J., *J. Am. Chem. Soc.* (2004) **126**, 4581-4595

[34] Ferenczi, M.A., Holmsher, E., Trentham, D.R., *J. Physiol.* (1984) **352**, 575-599

[35] Oksanen, E., unpublished

[36] Peng, L., Silman, I., Sussman, J., Goeldner, M., *Biochemistry* (1996) **35**, 10854-10861

[37] Morad, M., Goldman, Y.E., Trentham, D.R., *Nature* (1983) **304**, 635-638

[38] Wu, N., Deiters, A., Cropp, T.A., King, D., Schultz, P.G., *J. Am. Chem. Soc.* (2004) **126**, 14306-14307

[39] Gee, K.R., Kueper, L.W., Barnes, J., Dudley, G., Givens, R.S., *J. Org. Chem.* (1996) **61**, 1228-1233

[40] Ramesh, D., Wieboldt, R., Niu, L., Carpenter, B.K., Hess, G., *PNAS* (1993) **90**, 11074-11078

[41] Banerjee, A., Grewer, C., Ramakrishnan, L., Jäger, J., Gameiro, A., Breitinger, H-G.A., Gee, K.R., Carpenter, B.K., Hess, G.P., *J. Org. Chem.* (2003) **68**, 8361-8367

[42] Moffat, K., Henderson, R., *Curr. Opin. Struct. Biol*. (1995) **5,** 656-663

[43] Sawaya, M.R., Kraut, J., *Biochemistry* (1997) **36**, 586-603

[44] Heikinheimo, P., Tuominen, V., Ahonen, A.K, Teplyakov, A., Cooperman, B.S., Baykov, A.A., Lahti, R., Goldman, A., *PNAS* (2001) **98**, 3121-3126

[45] Tuominen, V., Heikinheimo, P., Kajander, T., Torkkel, T., Hyytiä, T., Käpylä, J., Lahti, R., Cooperman, B.S., Goldman, A., *J. Mol. Biol.* (1998) **284**, 1565-1580

[46] Ursby, T., Weik, M., Fioravanti, E., Delarue, M., Goeldner, M., Bourgeois, D., *Acta Cryst.* (2002) D**58**, 607-614

[47] Scott, W.G., Murray, J.B., Arnold, J.R.P., Stoddard, B.L., Klug, A. *Science* (1996) **274**, 2065-2069

[48] Teng, T., Moffat, K., *J. Appl. Cryst.* (1998) **31**, 252-257

[49] Ding, X., Rasmussen, B.F:., Petsko, G.A., Ringe, D., *Biochemistry* (1994) **33**(9), 9285-9293

[50] Blakeley, M.P., Cianci, M., Helliwell, J.R., Rizkallah, P.J., *Chem Soc Rev.* (2004) **33**(8), 548-557

[51] Blakeley, M.P., Kalb, A.J., Helliwell, J.R., Myles, D.A., *PNAS* (2004) **101**(47), 16405-16410

[52] Moffat, K., Szebenyi, D., Bilderback, D., *Science* (1984) **223,** 1423-1425

[53] Ren, Z., Bourgeois, D., Helliwell, J.R., Moffat, K., Srajer, V., Stoddard, B.L., *J. Synchrotron Rad.* (1999) **6**, 891-917

[54] Ren, Z., Moffat, K., *J. Appl.Cryst.* (1995) **28**, 482-493

[55] Nieh, Y.P., Raftery, J., Weisgerber, S., Habash, J., Schotte, F., Ursby, T., Wulff, M., Hädener, A., Campbell, J.W., Hao, Q., Helliwell, J.R., *J. Synchrotron Rad.* (1999) **6**, 995-1006

[56] Campbell, J.W., *J. Appl. Cryst.* (1995) **28**, 228-236

[57] Sweet, R.M., Singer, P.T., Smalås, A, *Acta Cryst.* (1998) D**49**, 305-307

[58] Ren, Z., Moffat, K., *J. Appl.Cryst.* (1995) **28**, 461-481

[59] Campbell, J.W., Hao, Q. *Acta Cryst.* (1993) A**49**, 889-893

[60] Terwilliger, T.C., Berendzen, J., *Acta Cryst.* (1995) D**51**, 609-618

[61] Ursby, T., Bourgeois, D., *Acta Cryst.* (1997) A**53**, 564-575

[62] Rajagopal, S., Schmidt, M., Anderson, M., Ihee, H., Moffat, K., *Acta Cryst.* (2004) D**60**, 860-871

[63] Srajer, V., Teng, T., Ursby, T., Praderwand, C., Ren, Z., Adachi, S., Schildkamp, W., Bourgeois, D., Wulff, M., Moffat, K., *Science* (1996) **274** 1726-1729

[64] Hummer, G., Schotte, F., Anfinrud, P.A., *PNAS* (2004) **101**(43) 15330-15334

[65] Schmidt, M., Pahl, R., Srajer, V., Aderson, S., Ren, Z., Ihee, H., Rajagopal, S., Moffat, K., *PNAS* (2004) **101**(14), 4799-4804

[66] Hajdu, J., Machin, P.A., Campbell, J.W., Greenhough, T.J., Clifton, I.J., Zurek, S., Gover, S., Johnson, L.N., Elder, M., *Nature* (1987) **329**, 178-181

[67] Duke, E.M.H., Wakatsuki, W., Hadfield, A., Johnson, L.N., *Protein Sci.* (1994) **3**, 1178-1196

[68] Schlichting, I., Almo, S.C., Rapp, G., Wilson, K., Petratos, K., Lentfer, A., Wittinghofer, A., Kabsch, W., Pai, E.F., Petsko, G.A., Goody, R.S., *Nature* (1990) **345**, 309-315

[69] Stoddard, B.L., Koenigs, P., Porter, N., Petratos, K., Petsko, G.A., Ringe, D., *PNAS* (1991) **88**, 5503-5507

[70] Bolduc, J.M., Dyer, D.H., Scott, W.G., Singer, P., Sweet, R.M., Koshland, D.E. Jr., Stoddard, B.L., *Science* (1995) **268**, 1312-1318

[71] Helliwell, J.R., Nieh, Y-P., Raftery, J., Cassetta, A., Habash, J.,Carr, P.D., Ursby, T., Wulff, M., Thompson, A.W., Niemann, A.C., Hädener, A., *J. Chem. Soc., Faraday Trans.* (1998) **94**(17) 2615-2622

[72] Koch, M.H., Vachette, P, Svergun, D.I., *Q. Rev. Biophys.* (2003) **36**(2), 147-227

[73] Svergun, D.I., Koch, M.H., *Curr. Opin. Struct. Biol.* (2002) **12**, 654-660

[74] Svergun, D.I., Volkov, V.V., Kozin, M.B., Stuhrmann, H.B., Barberato, C., Koch, M.H.J., *J. Appl. Cryst.* (1997) **30**, 798-802

[75] Svergun, D.I., Barberato, C., Koch, M.H.J., *J. Appl. Cryst.* (1995) **28**, 768-773

[76] Fetler, L., Vachette, P., *J. Mol. Biol.* (2001) **309**, 817-832

[77] Amenitsch, H., Rappolt, M., Kriechbaum, M., Mio, H., Laggner, P., Bernstorff, S., *J. Synchrotron Rad.* (1998) **5**, 506-508

[78] Segel, D.J., Elizier, D., Uversky, V., Fink, A.L., Hodgson, K.O., Doniach, S., *Biochemistry* (1999) **38**, 15352-15359

[79] Svergum, D.I., Nierhaus, K.H., *J. Biol. Chem.* (2000) **275**, 14432-14439

[80] Schluenzen, F., Tocilj, A., Zarivach, R., Harms, J., Gluehmann, M., Janell, D., Bashan, A., Bartels, H., Agmon, I., Franceschi, F., Yonath, A., *Cell* (2000) **102**, 615-623

[81] Cavanagh, J. *Protein NMR spectroscopy: priciples and practice*, Academic Press (1996) San Diego, USA

[82] Eisenmesser, E.Z., Bosco, D.A., Akke, M., Kern, D., *Science* (2002) **295**, 1520-1523

[83] Wang, L., Pang, Y., Holder, T., Brender, J.R., Kurochkin, A.V., Zuiderweg, E.R.P., *PNAS* (2001) **98**, 7684-7689